Accepted 12th June 2017

A biocatalytic and thermoreversible hydrogel from a histidine-containing tripeptide†

A. M. Garcia,‡[a] M. Kurbasic, ‡[a] S. Kralj, [ab] M. Melchionna[a] and S. Marchesan *[a]

We report the first histidine-containing self-assembling tripeptide devoid of capping groups that forms a thermoreversible hydrogel under physiological conditions and catalyses hydrolysis of an ester, providing a minimalist building block for functional soft materials.

Short peptides have emerged as very attractive minimalist building blocks for supramolecular (bio)materials, in light of their simplicity of preparation and benign fate in biological settings and in the environment.[1] The vast majority of these systems exploit synthetic N-capping groups that are rigid and aromatic (*e.g.*, Fmoc, Nap, *etc.*), thus effectively templating self-assembly.[2] Recently, useful tools have been developed to predict their gelation.[3] In the case of unprotected (tri)peptides, *a priori* self-assembly design in water is notoriously difficult. Despite intense research efforts have enabled the development of valid tools to predict their aggregation propensity,[4–6] very few hydrogel examples have been reported thus far. The first unprotected tripeptides self-assembling into hydrogels were described in 2012 and consisted of hydrophobic sequences that exploited appropriate positioning of D- and L-amino acids in heterochiral sets of three.[7,8] The key role played by the amino acid stereoconfiguration was confirmed in a complete stereoisomer series whereby homochiral analogues did not assemble.[9,10] In 2015, the first four L-tripeptides able to gel were reported, consisting of amphiphilic sequences bearing a hydrophilic lysine and two aromatic amino acids (*i.e*, Phe, Tyr, and/or Trp).[5] Another four examples soon followed bearing amino acids Glu, Thr, Lys or Cys besides aromatic Phe residues; however, they all required small amounts (*i.e.*, 8%) of an organic solvent to assist the dissolution, and the final pH of the hydrogel was below 5, thus limiting biological use.[11] Considering that hydrogels formed by unprotected tripeptides may also disassemble at mild temperatures around 30 °C, it is apparent how the formation of stable biomaterials from these building blocks is far from trivial.[10]

Here we report the first example of an unprotected tripeptide bearing His forming a supramolecular hydrogel under physiological conditions. The hydrogel withstands temperatures used in cell culture for potential use as a biomaterial, is thermoreversible, and catalyses ester hydrolysis, thus showing potential towards functional soft materials.

^{L}His–^{D}Phe–^{D}Phe formed a thermoreversible hydrogel at 2 wt% in phosphate buffer following a pH trigger to neutral at room temperature (Fig. 1). The gel-to-sol transition had an onset temperature of 45 °C, as observed visually and confirmed by differential scanning calorimetry (DSC). A homogeneous

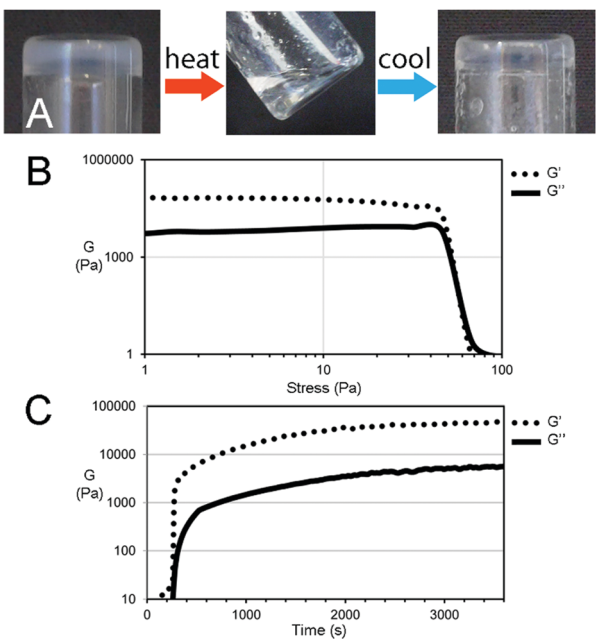

Fig. 1 (A) Thermoreversible peptide gels. (B) Hydrogel stress sweep. (C) Gelation kinetics.

[a] *Dip. Sc. Chim. Farm., University of Trieste, Via L. Giorgieri 1, 34127 Trieste, Italy. E-mail: smarchesan@units.it, marchesan.silvia@gmail.com*

[b] *Materials Synthesis Department, Jožef Stefan Institute, Jamova 39, 1000 Ljubljana, Slovenia*

‡ These authors contributed equally to this work.

solution was obtained at 65 °C and the gel reformed after *ca.* 10 minutes upon cooling to room temperature (Fig. 1A). DSC data confirmed a wide endotherm for the gel-to-sol transition, however, with a remarkably high T_m = 88–90 °C (see the ESI†). This temperature is compatible with that of the amyloid nanostructure disassembly, as recently reviewed.[12] While gel melting implies the loss of the three-dimensional network forming the gel matrix, it does not necessarily correspond to a complete loss of the amyloid nanostructure, which typically occurs at higher temperatures.

The viscoelastic properties of the system were assessed by rheometry that revealed good resistance to applied stress for the peptide gel, since the gel-to-sol transition was observed at 50 Pa (Fig. 1B). The elastic modulus was also considerably high for an unprotected tripeptide, and reached 50 kPa and beyond as the self-assembly proceeded over time (Fig. 1C).

FT-IR, Thioflavin T fluorescence assay, and CD were employed to assess the peptide conformation (Fig. 2 and the ESI†). The amide I band region in the FT-IR spectra is very informative of the secondary structure, with beta-sheets most frequently reported for self-assembled short peptides.[13,14] In the case of His–Phe–Phe hydrogels, the spectra displayed a signal compatible with the beta-sheets (1637 cm^{-1}) as typically occurs for similar amyloid peptides,[10] although it was not possible to discern the presence of the characteristic shoulder for the anti-parallel arrangement, due to the intense signal of the TFA counterion (1677 cm^{-1}). In addition, the presence of other maxima at 1653 cm^{-1} and 1600 cm^{-1} suggested a certain level of heterogeneity in the peptide secondary structure (Fig. 2A), which is compatible with the wide gel-to-sol endotherm observed by DSC. The amide II band region was dominated by a broad signal centred at 1545 cm^{-1} and a shoulder at 1514 cm^{-1}. The amyloid structure based on beta-sheets was also confirmed by the Thioflavin T fluorescence assay (see the ESI†). The dye is known to bind laterally to amyloid fibrils composed of at least four consecutive beta-strands.[15] This interaction limits the rotation of a single bond that connects the two aromatic rings that compose the dye, resulting in fluorescence.[16]

CD was also used to monitor the peptide conformation, as the region of 190–220 nm is indicative of the secondary structure. However, the concentration required for self-assembly led to signal saturation below 220 nm even when 0.1 mm cuvettes were used. Nevertheless, the acquisition of CD spectra in the 220–300 nm region over time proved to be useful to monitor the self-assembly (Fig. 2B). Ellipticity evolved during the first 20 minutes until it reached a plateau. A negative minimum at 225 nm suggested the D-supramolecular chirality as previously observed for heterochiral unprotected tripeptides.[10] The spectrum was also characterised by a shoulder at 230–240 nm. In the near-UV region of 255–270 nm, the weak but distinctive signal of vibronic states for the forbidden $\pi \rightarrow \pi^*$ transition of the aromatic ring indicated that Phe side chains were located in a chiral environment.[17]

Atomic force microscopy (AFM) and transmission electron microscopy (TEM) were used to visualise nanomorphological features of peptide assemblies (Fig. 3). The hydrogel was formed by a dense network of bundles of fibres reaching a thickness of over 1 micron, and as long as tens of microns, thus explaining the high elastic modulus registered by rheometry.

Next, the catalytic function of the hydrogel was assessed. In recent years, there has been an increasing interest in the development of minimalist peptide motifs for biocatalysis. In particular, esterase-mimicking motifs have been the most studied ones, and typically employ sequences containing either the Ser–His–Asp catalytic triad or the His–Zn^{2+} coordination motif. While His alone does not exhibit catalytic activity, it is the most important amino acid playing the role of a proton donor or acceptor in ester hydrolysis.[18] The supramolecular organisation of His-bearing peptides is a strategy that can successfully achieve biocatalysis through the creation of multivalency, typically featuring ordered arrays of His residues. While initial reports displayed peptides as long as 42 amino acids,[19,20] research efforts have ever since been devoted towards the development of conveniently shorter sequences. To date, this approach has been proven to be successful for nanofibers formed by decapeptide amphiphiles,[21] capped 14-mer[22] and 7-mer[23,24] peptides, and even *N*-acetylated pentamers assembled on the surface of gold nanoparticles.[25] This minimalist approach culminated with Fmoc–tripeptide nanotubes.[26] However, all these examples feature peptides derivatised at either one or both termini, likely due to the intrinsic difficulties of the self-assembly design for unprotected short peptides. Besides, it should be noted that catalysis by means of isolated nanostructures in solution is markedly different from the catalysis occurring in bulk functional materials.

To test for catalytic activity, we employed a colourimetric screen based on *p*-nitrophenylacetate (pNPA) hydrolysis to generate

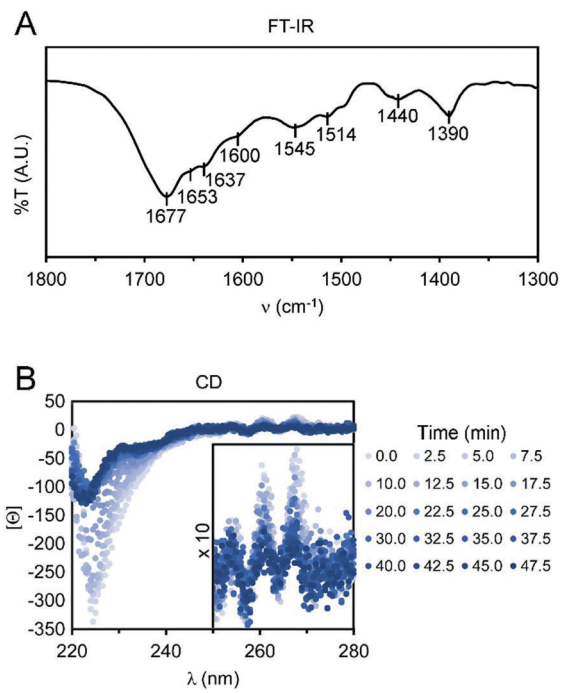

Fig. 2 (A) FT-IR spectrum (amide I–II region). (B) CD spectra over time during gelation.

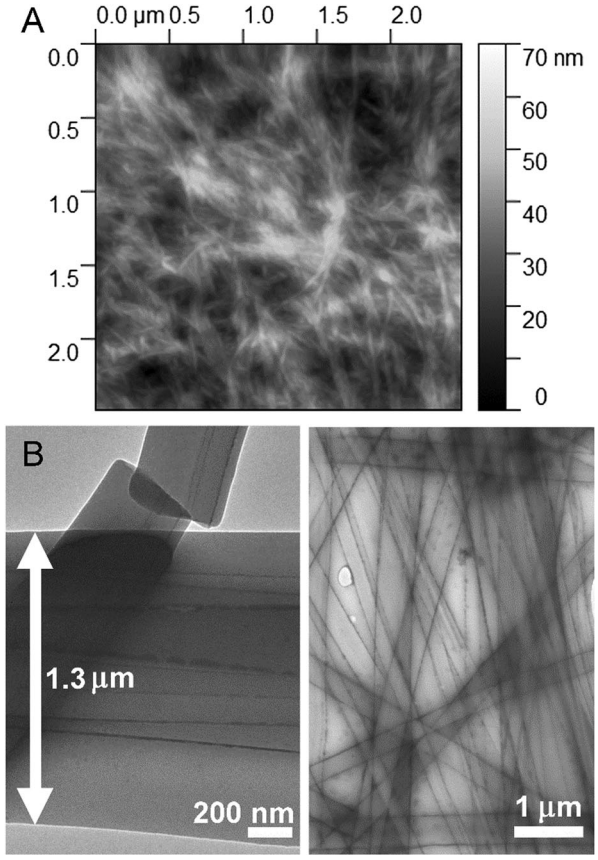

Fig. 3 (A) AFM image of peptide hydrogel. (B) TEM image at high (left) and low (right) magnifications of the peptide hydrogel.

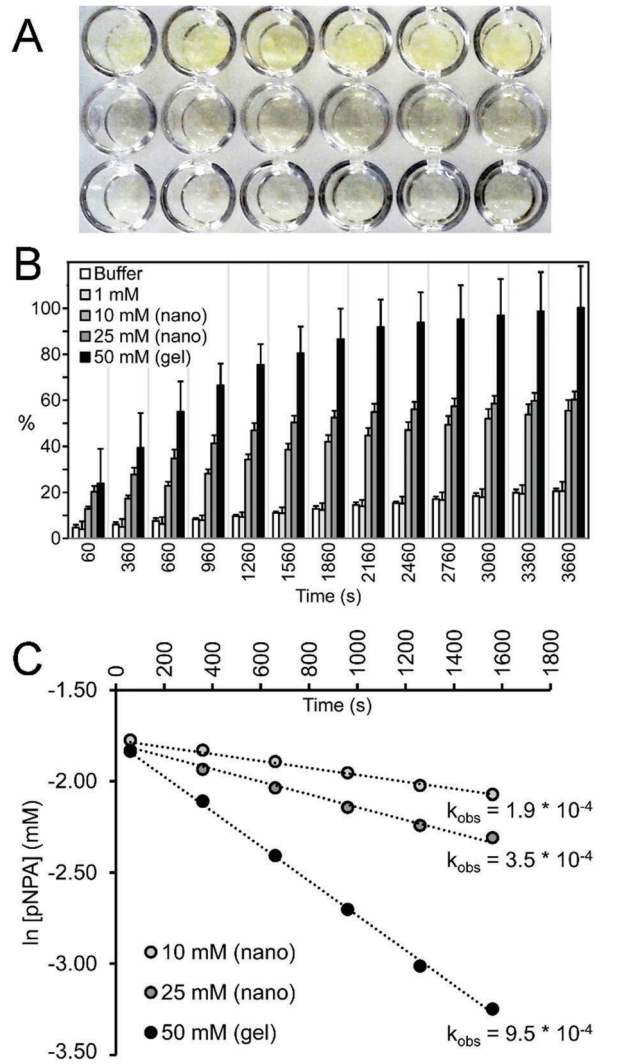

Fig. 4 (A) Multi-well plate colourimetric screen for ester hydrolysis. (B) Substrate conversion into product over time and at different peptide concentrations. (C) Esterase-like activity observed rate (k_{obs}) for the catalytic peptide systems. Note: (nano) refers to formation of nanostructures, while (gel) refers to the hydrogel system.

the yellow-coloured *p*-nitrophenol (pNP) that is easily quantified by measuring the absorbance at 405 nm.[27] The product formation was monitored over one hour (Fig. 4 and the ESI†), and it was negligible for control samples with 1 mM peptide solution or buffer (k_{obs} = 5.0 × 10^{-5} s^{-1} in both cases). By contrast, the presence of the supramolecular hydrogel resulted in marked biocatalysis (k_{obs} = 9.5 × 10^{-4} s^{-1} increased to 1.7 × 10^{-3} s^{-1} with 1 mM pNPA), and that reached a plateau corresponding to complete conversion of the substrate into the product, and visibly yellow gels. Intermediate peptide concentrations that were below mgc displayed moderate catalysis (Fig. 4C) and absence of a linear dependence of k_{obs} on the peptide concentration. TEM analysis (see the ESI†) revealed the presence of thin nanofibrils (10 mM sample) and also oligomers and protofibrils (25 mM sample), which are typical morphologies of early-stage amyloid assemblies.[28,29] Overall, these results confirmed that the esterase-like activity is associated with the formation of supramolecular structures.

In conclusion, we reported herein the first unprotected tripeptide bearing His and forming supramolecular hydrogels under physiological conditions. In the context of unprotected tripeptide hydrogels, this is the first example displaying a catalytic function, thus setting a new benchmark in the quest for minimalist biocatalysts. The material is thermoreversible at temperatures higher than those used in cell culture, allowing potential use as a biomaterial and offering the opportunity to control assembly and disassembly by heating/cooling, besides changing of pH values. Further studies in this area will provide simple building blocks for supramolecular functional biomaterials.[30] If the field advances towards a catalytic function with a higher level of complexity, an appropriate choice of amino acid chirality may also offer interesting opportunities towards stereoselective reactions.

The authors would like to acknowledge funding from the Italian Ministry of University and Research (MIUR) through the SIR program (''HOT-SPOT'' project, personal research grant n. RBSI14A7PL for SM), Ramón Areces Foundation (AMG fellowship), and European Social Fund Operational Programme 2014–2020 (Axis 3 – Education and Training, Specific Programme no. 26 – TALENTS^3 – SK fellowship). The authors also acknowledge the use of equipment at the Center of Excellence on Nanoscience and Nanotechnology at Jožef Stefan Institute.

References

1 A. Dasgupta, J. H. Mondal and D. Das, *RSC Adv.*, 2013, **3**, 9117–9149.
2 X. Du, J. Zhou, J. Shi and B. Xu, *Chem. Rev.*, 2015, **115**, 13165–13307.
3 J. K. Gupta, D. J. Adams and N. G. Berry, *Chem. Sci.*, 2016, **7**, 4713–4719.
4 T. Tuttle, *Isr. J. Chem.*, 2015, **55**, 724–734.
5 P. W. Frederix, G. G. Scott, Y. M. Abul-Haija, D. Kalafatovic, C. G. Pappas, N. Javid, N. T. Hunt, R. V. Ulijn and T. Tuttle, *Nat. Chem.*, 2015, **7**, 30–37.
6 P. W. J. M. Frederix, R. V. Ulijn, N. T. Hunt and T. Tuttle, *J. Phys. Chem. Lett.*, 2011, **2**, 2380–2384.
7 S. Marchesan, L. Waddington, C. D. Easton, D. A. Winkler, L. Goodall, J. Forsythe and P. G. Hartley, *Nanoscale*, 2012, **4**, 6752–6760.
8 S. Marchesan, C. D. Easton, F. Kushkaki, L. Waddington and P. G. Hartley, *Chem. Commun.*, 2012, **48**, 2195–2197.
9 A. V. Vargiu, D. Iglesias, K. E. Styan, L. J. Waddington, C. D. Easton and S. Marchesan, *Chem. Commun.*, 2016, **52**, 5912–5915.
10 S. Marchesan, K. E. Styan, C. D. Easton, L. Waddington and A. V. Vargiu, *J. Mater. Chem. B*, 2015, **3**, 8123–8132.
11 S. Zarzhitsky, T. P. Vinod, R. Jelinek and H. Rapaport, *Chem. Commun.*, 2015, **51**, 3154–3157.
12 K. Sasahara and Y. Goto, *Biophys. Rev.*, 2013, **5**, 259–269.
13 S. Fleming, P. W. J. M. Frederix, I. Ramos Sasselli, N. T. Hunt, R. V. Ulijn and T. Tuttle, *Langmuir*, 2013, **29**, 9510–9515.
14 M. Melchionna, K. E. Styan and S. Marchesan, *Curr. Top. Med. Chem.*, 2016, **16**, 2009–2018.
15 J. E. Shea, C. Wu, M. Biancalana and S. Koide, *J. Mol. Biol.*, 2009, **394**, 627–633.
16 N. Amdursky, Y. Erez and D. Huppert, *Acc. Chem. Res.*, 2012, **45**, 1548–1557.
17 Z. Li and J. D. Hirst, *Chem. Sci.*, 2017, **8**, 4318–4333.
18 K. L. Duncan and R. V. Ulijn, *Biocatalysis*, 2015, **1**, 67–81.
19 K. S. Broo, L. Brive, P. Ahlberg and L. Baltzer, *J. Am. Chem. Soc.*, 1997, **119**, 11362–11372.
20 L. Baltzer, K. S. Broo, H. Nilsson and J. Nilsson, *Bioorg. Med. Chem.*, 1999, **7**, 83–91.
21 M. O. Guler and S. I. Stupp, *J. Am. Chem. Soc.*, 2007, **129**, 12082–12083.
22 C. Zhang, X. Xue, Q. Luo, Y. Li, K. Yang, X. Zhuang, Y. Jiang, J. Zhang, J. Liu, G. Zou and X.-J. Liang, *ACS Nano*, 2014, **8**, 11715–11723.
23 C. M. Rufo, Y. S. Moroz, O. V. Moroz, J. Stöhr, T. A. Smith, X. Hu, W. F. DeGrado and I. V. Korendovych, *Nat. Chem.*, 2014, **6**, 303–309.
24 C. Yang, H. Wang, D. Li and L. Wang, *Chin. J. Chem.*, 2013, **31**, 494–500.
25 D. Zaramella, P. Scrimin and L. J. Prins, *J. Am. Chem. Soc.*, 2012, **134**, 8396–8399.
26 Z. Huang, S. Guan, Y. Wang, G. Shi, L. Cao, Y. Gao, Z. Dong, J. Xu, Q. Luo and J. Liu, *J. Mater. Chem. B*, 2013, **1**, 2297–2304.
27 U. T. Bornscheuer, *Eng. Life Sci.*, 2004, **4**, 539–542.
28 M. Ahmed, J. Davis, D. Aucoin, T. Sato, S. Ahuja, S. Aimoto, J. I. Elliott, W. E. Van Nostrand and S. O. Smith, *Nat. Struct. Mol. Biol.*, 2010, **17**, 561–567.
29 H. A. Lashuel, D. M. Hartley, B. M. Petre, J. S. Wall, M. N. Simon, T. Walz and P. T. Lansbury Jr, *J. Mol. Biol.*, 2003, **332**, 795–808.
30 J. Zhou, J. Li, X. Du and B. Xu, *Biomaterials*, 2017, **129**, 1–27.